Annals of Biomedical Engineering, Vol. 33, No. 6, June 2005 (© 2005) pp. 751–763
DOI: 10.1007/s10439-005-3236-2

The Effect of Conductivity on ST-Segment Epicardial Potentials Arising from Subendocardial Ischemia

BRUCE HOPENFELD,[1,2] JEROEN G. STINSTRA,[1,2] and ROB S. MACLEOD[1,2]

[1]The Nora Eccles Harrison Cardiovascular Research and Training Institute, University of Utah, Salt Lake City, Utah 84112-5000 and [2]Bioengineering Department at the University of Utah and the Scientific, Computing and Imaging Institute at the University of Utah

(Received 10 August 2004; accepted 27 January 2005)

Abstract—We quantify and provide biophysical explanations for some aspects of the relationship between the bidomain conductivities and ST-segment epicardial potentials that result from subendocardial ischemia. We performed computer simulations of ischemia with a realistic whole heart model. The model included a patch of subendocardial ischemic tissue of variable transmural thickness with reduced action potential amplitude. We also varied both intracellular and extracellular conductivities of the heart and the conductivity of ventricular blood in the simulations. At medium or high thicknesses of transmural ischemia (i.e., at least 40% thickness through the heart wall), a consistent pattern of two minima of the epicardial potential over opposite sides of the boundary between healthy and ischemic tissue appeared on the epicardium over a wide range of conductivity values. The magnitude of the net epicardial potential difference, the epicardial maximum minus the epicardial minimum, was strongly correlated to the intracellular to extracellular conductivity ratios both along and across fibers. Anisotropy of the ischemic source region was critical in predicting epicardial potentials, whereas anisotropy of the heart away from the ischemic region had a less significant impact on epicardial potentials. Subendocardial ischemia that extends through at least 40% of the heart wall is manifest on the epicardium by at least one area of ST-segment depression located over a boundary between ischemic and healthy tissue. The magnitude of the depression is a function of the bidomain conductivity values.

Keywords—Ischemia, ST depression, Conductivity, Computer model.

INTRODUCTION

ST-segment depression and elevation remain important electrocardiographic tools for diagnosing myocardial ischemia despite incomplete understanding of their biophysical basis and clinical interpretation. We have previously proposed a mechanism, based on the anisotropic conductivity of heart tissue, for the sources and spatial organization of ST-segment potentials.[2] Omitted from this study, however, was a detailed characterization of the relationship between tissue conductivity and epicardial potentials during the ST segment. The motivation for such a study comes first from the wide range of values proposed for myocardial tissue conductivity[9] and, perhaps more importantly, because these values are known to fluctuate as functions of the degree and time course of ischemia.[9] Thus, there may be variations in the electrocardiogram (ECG) in patients with ischemia that are not related to a true change in the extent or degree of ischemia but rather to changes only in tissue conductivity. Hence, a full understanding of the relationship between tissue conductivity and electrocardiographic response is essential.

There are two distinct components that determine the electrocardiographic response to myocardial ischemia and our studies addressed them both. First, at the boundary between ischemic and healthy tissue there are localized transmembrane potential differences; these are the ischemic sources. The sources arise because of differences in transmembrane potential across this ischemic boundary, and the resulting epicardial potentials reflect the magnitude, shape, and location of these sources within the anisotropic heart. More specifically, the local alignment of intracellular and extracellular potential gradients with myocardial fiber orientation will result in potential differences that lead ultimately to epicardial elevations and depressions organized around the ischemic region. The second component of the bioelectric response to ischemia is the passive electrical load that the tissues outside the sources—the volume conductor—place on the sources. The volume conductor consists of a combination of the extracardiac torso and that region of the heart that is remote from the ischemic zone. Conductivity of the volume conductor determines how current flows through it and determines the electric potentials that develop on the body surface (the ECG).

Both our previous findings[2] and experimental and modeling results by Li *et al*.[4] suggest that in the case of subendocardial ischemia, maximal epicardial ST depression occurs over a lateral boundary between normal and ischemic tissue. (As shown in Fig. 1, assuming an approximately rectilinear ischemic region, there are four lateral boundaries between

Address correspondence to Bruce Hopenfeld, National Heart Lung & Blood Institute, National Institutes of Health, 10 Center Drive, MSC 1061, Bethesda, Maryland 20892-1061. Electronic mail: brhopenfeld@yahoo.com

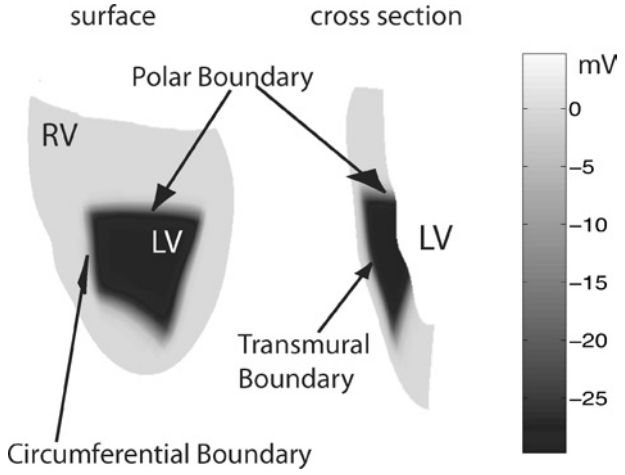

FIGURE 1. Transmembrane potential distribution over a midmyocardial layer and a sagittal slice showing an anterior, subendocardial ischemic zone. The transmembrane potential of the ischemic patch was negative with respect to the transmembrane potential of the healthy tissue, as indicated by the scale. The polar and circumferential lateral boundaries and the transmural boundary are indicated by arrows.

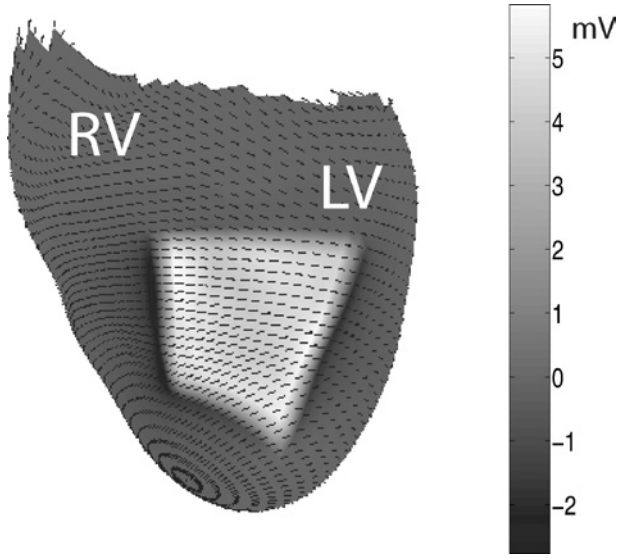

FIGURE 2. Extracellular potential distribution on an internal heart layer, showing the effect of fiber orientation on the potential difference across the ischemic boundary (indicated by the positive potential values). Fiber direction is indicated by arrows.

healthy and ischemic tissue, two of which mark the circumferential extent of the ischemic region and align with radial lines from the anatomic central axis of the ventricle, and two of which lie parallel to the base of the heart and mark the caranial-caudal extent of ischemia. There are two transmurally oriented boundaries, one adjacent to the ventricular blood mass and the other parallel to the epicardium.)

Our results suggest that the lateral areas of epicardial ST-segment depression originate from the difference between the electrical conductivity along heart muscle fiber direction (longitudinal) and the electrical conductivity transverse to fiber direction. Specifically, the ratio of intracellular conductivity to extracellular conductivity (σ_i/σ_e) along fibers is greater than the same ratio transverse to fibers.[9] Because the extracellular potential difference across an ischemic boundary is an increasing function of σ_i/σ_e,[2] the extracellular potential difference across an ischemic boundary tends to be greater where the boundary is crossed along fibers than where the boundary is crossed transverse to fibers. Figure 2 shows extracellular potential on a midmyocardial layer of ischemic tissue. From this figure, one can observe the variation in spatial potential gradient across the four visible lateral borders; where the fibers are perpendicular to the lateral ischemic boundary, the potential gradient is relatively large. Conversely, where the fibers are parallel to the lateral boundary, the potential gradient is relatively small.

Because at least some components of the lateral boundary tend to be perpendicular to the fiber direction, the resulting extracellular potential gradient tends to be relatively large across those lateral boundaries. Conversely, because transmural ischemic boundaries tend to be parallel to fiber direction, the extracellular potential gradient tends to be relatively small across these transmural boundaries. As a consequence of this spatial organization of potential gradients, and as shown in Fig. 3, injury currents tend to flow in loops from the ischemic side of the lateral borders toward the transmural borders, and then return through the healthy tissue volume, passing along the epicardium in a direction that generates ST-segment elevation in the region above the ischemic zone and ST-segment depression over its lateral boundaries.

Our previous findings thus suggest that the epicardial potential distribution depends on the relative magnitude of the potential differences across the lateral ($\Delta V_{e,lat}$) and transmural ($\Delta V_{e,tm}$) boundaries. (The "e" in the subscripts for $\Delta V_{e,lat}$ and $\Delta V_{e,tm}$ indicates that these voltage differences are in the extracellular space.) As shown schematically in the upper panels of Fig. 3, $\Delta V_{e,lat}$ and $\Delta V_{e,tm}$ act as potential sources for the resulting injury currents. The lower panel of Fig. 3 also shows how the potential sources depend on the geometry of the ischemic region, the difference in transmembrane potentials between normal and ischemic regions, and the bidomain conductivities, i.e., the value of σ_i/σ_e along and transverse to fibers. The relationship between these parameters and the potential source distribution is governed by the bidomain passive current flow equation:

$$\nabla \cdot (\bar{\sigma}_i + \bar{\sigma}_e)\nabla V_e = -\nabla \cdot \bar{\sigma}_i \nabla V_m, \qquad (1)$$

where V_e is the extracellular potential, $\bar{\sigma}_i$ is the intracellular conductivity tensor, $\bar{\sigma}_e$ is the extracellular conductivity tensor, and V_m is the transmembrane potential. The right hand side of Eq. (1) defines the current sources and sinks across

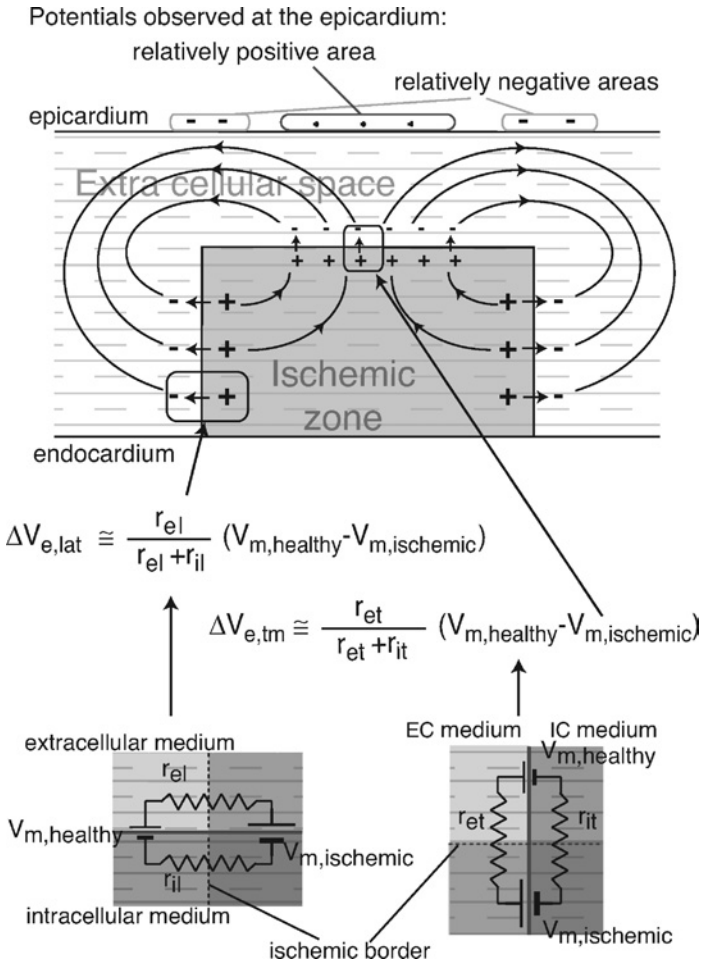

FIGURE 3. Current flow and potential differences in an ischemic heart. The potential drop across the lateral ischemic boundary is greater than the potential drop across the transmural boundary, as indicated by the size of the + and − symbols. Most current flows directly across the ischemic boundary, as indicated by the thick arrows. However, a small amount of current flows in a loop from the lateral ischemic boundary, through the ischemic tissue, across the transmural boundary and thence to the healthy tissue on the lateral boundary. The potential difference ΔV_e is greater across the lateral than transmural boundary due to the difference in resistances of the two boundaries.

an ischemic boundary. These current sources are depicted by the straight arrows across the boundary shown in Fig. 3.

According to Eq. (1), the voltage source across an ischemic boundary may be approximated by the multiplication of current density flowing across the boundary $\bar{\sigma}_i \nabla V_m$, multiplied by the resistivity across the boundary $(\bar{\sigma}_i + \bar{\sigma}_e)^{-1}$, resulting in voltage divider equations for the lateral and transmural boundaries as follows:

$$\Delta V_{e,lat} \approx \frac{\Delta V_m}{1 + \sigma_{el}/\sigma_{il}} \tag{2}$$

$$\Delta V_{e,tm} \approx \frac{\Delta V_m}{1 + \sigma_{et}/\sigma_{it}}, \tag{3}$$

where ΔV_m, is the transmembrane potential difference across the ischemic boundary, i.e., the difference in transmembrane potential between ischemic and healthy tissue, σ_{el} and σ_{il} are the longitudinal extracellular and intracellular conductivities, respectively, and σ_{et} and σ_{it} are the transverse extracellular and intracellular conductivities. Roberts *et al.*[8] used these equations to estimate the conductivity ratios σ_{el}/σ_{il} and σ_{et}/σ_{it} based upon the epicardial potential drops measured across a wave front. These equations may also be derived by considering ΔV_m as a battery, as shown in the lower panel of Fig. 3. (The resistances in the figure are the inverses of the bidomain conductivities, adjusted for length and cross sectional area.) Since ΔV_m is constant across the entire ischemic boundary, the values of σ_e/σ_i for the intracellular and extracellular spaces determine the strength of the voltage sources.

The contribution of the bidomain conductivities to the distribution of potentials in the heart is not, however, limited to the source potentials. A second role of these values is to

characterize the volume conductor into which the resulting injury currents flow. We will use the terms "voltage source effects" to describe the role of conductivity in determining the ischemic potential sources and "secondary volume conductor effects" to describe the secondary role of conductivity in determining the distribution of the resulting injury currents. The combination of these two contributions ultimately determines the resulting epicardial potentials.

Our previous studies[2] did not attempt to quantify the relationship among potential source effects, secondary volume conductor effects and epicardial potentials. The aims of this study were to describe and provide biophysical explanations of this relationship and, in addition, to evaluate the contribution of ventricular blood to epicardial potential distributions during ischemia. Toward this end, we carried out computer simulations on a fully anisotropic model of the left and right ventricles; we varied the conductivity of heart tissue and blood to determine the relationship between these parameters and epicardial potentials.

The primary findings of this study are that the basic topography of epicardial potential patterns generally did not change as a function of conductivity, but that the magnitudes of epicardial potentials are sensitive to the conductivity values, mainly through voltage source effects.

The significance of this research lies in the need to understand the biophysical basis for the currents and potentials that arise during myocardial ischemia and the role that tissue conductivity plays in those bioelectric markers. Ultimately, this understanding may lead to better interpretation of body surface ECG changes that arise during subendocardial ischemia and hence improvements in diagnosis and monitoring of patients suffering from coronary artery disease.

METHODS

Geometric Model

We simulated ischemia by using a geometric model based on the anatomical and fiber structure data of the Auckland canine heart.[7] The computer model solved the equation governing the passive flow of current in the heart, according to the bidomain theory [Eq. (1)], given a distribution of transmembrane potentials. To represent the electrical consequences of localized acute ischemia, we assigned to a patch of tissue transmembrane potentials that were 30 mV more negative than in the remaining healthy cells, as shown in Fig. 1, which depicts the transmembrane potentials corresponding to 70% transmural ischemia. The goal of this arrangement was to mimic the conditions during the electrocardiographic ST-segment, which corresponds to the plateau phase of the action potential; ischemic cells show a reduced action-potential amplitude that results in a more negative plateau potential than the surrounding healthy tissue. The ischemic patch was placed within the left ventricular free wall with a border zone between healthy and ischemic tissue that was a few millimeters wide. Within this border zone, the transmembrane potential varied smoothly from -30–0 mV according to an exponential function.[3] The size of the ischemic patch was altered in the transmural direction to simulate various degrees of subendocardial ischemia.

The anatomy of the Auckland heart, including ventricles filled with blood, was represented with a hexahedral mesh defined by a number of nested, concentric layers with identical numbers and arrangements of node points. The ventricles consisted of 60 such layers that were weighted averages of the epicardial and endocardial surfaces. For example, the 30th layer was equal to approximately $0.5 \times \text{Epi} + 0.5 \times \text{Endo}$, where Epi and Endo were the Cartesian coordinates that defined the epicardial and endocardial surfaces, respectively. The degree of ischemia was defined with respect to the 60 layers. For example, 40% ischemia means that the ischemia extended from the endocardium to the 24th layer. Included in the Auckland heart data are also values for the local fiber orientation, which were assigned to each node point in the geometry. The resulting mesh then served as the geometric domain over which we solved the bidomain passive current flow equation, Eq. (1).

With regard to boundary conditions, the heart was assumed to be surrounded by a perfect insulator so that no current could flow out of the epicardial surface. At any interface between ventricular blood and heart muscle, the extracellular potential V_e was continuous, the normal component of the extracellular current was continuous, and no intracellular current could flow across the interface. Equation (1) was solved according to a Galerkin-based finite element method with trilinear basis functions and Gauss quadrature to integrate the resulting equations. The conductivity tensor at each quadrature point was based on the local fiber orientation, which was computed by forming a distance-based weighted average of the fiber orientation data corresponding to the eight nearest points from the Auckland data.

Simulations

The values of cardiac tissue conductivity (i.e. the intracellular and extracellular conductivity tensors in Eq. (1)) are uncertain.[9] Our model of cardiac tissue[9] suggests that the values for the various conductivities are within the ranges shown in Table 1. Of the four conductivity ratios that describe heart tissue (σ_{il}/σ_{el}, σ_{it}/σ_{et}, σ_{il}/σ_{it}, and σ_{el}/σ_{et}) only three can be changed independently. The fourth conductivity will always depend on the choice of some combination of the other three. In our simulations, we chose σ_{il}/σ_{el}, σ_{il}/σ_{et}, and σ_{el}/σ_{et} as the independent variables,

TABLE 1. Conductivity ranges computed from a model of cardiac myocytes.

Parameter	Symbol	Values
Longitudinal extracellular conductivity	σ_{el}	**1**
Ratio of longitudinal intracellular to longitudinal extracellular conductivity	σ_{il}/σ_{el}	0.2 0.6 **1** 2 3
Intracellular anisotropy ratio	σ_{il}/σ_{it}	**20** 30 40 50
Extracellular anisotropy ratio	σ_{el}/σ_{et}	1 **3** 5
Blood conductivity	σ_b/σ_{el}	2 **3** 4

Note. σ_{il}/σ_{it} is the intracellular anisotropy ratio, σ_{el}/σ_{et} is the extracellular anisotropy ratio, and σ_b/σ_{el} is the blood conductivity ratio. For convenience, all ratios are normalized to an extracellular longitudinal conductivity, σ_{el}, of 1. The baseline conductivity values are indicated in bold.

while σ_{it}/σ_{et} was left as the dependent ratio, and therefore changes in step with alterations of any of the independent ratios. For example, a doubling of σ_{it}/σ_{et} results in a doubling of σ_{il}/σ_{el}. σ_{il}/σ_{el} should thus be viewed as a parameter that controls the overall ratio of intracellular to extracellular conductivity (i.e. it affects both σ_{il}/σ_{el} and σ_{it}/σ_{et}).

In a first set of simulations, the bidomain and ventricular blood conductivities were varied as shown in Table 1 at each of 10, 40, and 70% ischemia, corresponding to low, medium, and high degrees, respectively, of subendocardial ischemia. The ischemic and healthy portions of the heart were assigned identical conductivity values. We chose 10, 40, and 70% ischemia to be consistent with a previous conductivity sensitivity study.[3] For each degree of ischemia, we generated simulations for each combination of conductivity ratios shown in Table 1, for a total of $5 \times 4 \times 3 \times 3 = 180$ simulations for each degree of ischemia. The result of each simulation was a three-dimensional distribution of extracellular potentials voltage.

To help distinguish source effects from secondary volume conductor effects, we carried out simulations under two different baseline conditions at both 40 and 70% ischemia. In both simulations, conditions within the ischemic zone matched the baseline values shown in Table 1. In the first case, these same conditions held throughout the rest of the heart volume and in the second case, we assigned uniform, isotropic conditions to all regions outside of the ischemic zone. The tissue outside of the ischemic zone was assigned the following conductivities: $\sigma_{el} = \sigma_{il} = \sigma_{et} = \sigma_{it} = 1/3$. Thus, the first set of simulations included the effects of anisotropy of both the source and the surrounding myocardium. The second set of simulations, in contrast, included the effects only of anisotropy in the source conductivity. To evaluate the effect of blood volume on ischemic potentials, we carried out simulations both with insulated ventricular cavities and with the ventricles filled with conductive blood.

RESULTS

Conductivity Sensitivity

Figures 4, 5, and 6 show the epicardial potential distributions corresponding to a selection of conductivity values from Table 1 at 10%, 40%, and 70% transmural ischemia, respectively. To isolate the effect of changes in particular parameter values, for each parameter that was varied, we held all the remaining parameters equal to the baseline values shown in bold in Table 1. As discussed in Section II-B, the ratio σ_{il}/σ_{el} controlled the overall intracellular to extracellular conductivity.

A comparison of Figs. 5 and 6 shows that the epicardial potential patterns at 40% ischemia were similar to those at 70% except for three features. First, the magnitudes at 40% were smaller than those at 70%. Second, the relative minima at 40% were rotated counterclockwise compared to the minima at 70%. Finally, at large values of the extracellular anisotropy ratio (e.g., $\sigma_{el}/\sigma_{et} = 5$), the maximum shifted from over the ischemic patch to over a circumferential lateral boundary.

The epicardial distributions at 10% ischemia were quite different from those at 70% ischemia. Specifically, at 10% ischemia, ST depression was centered over the ischemic patch while at 70% ischemia, potentials over the ischemic patch were elevated and regions of ST depression appeared over the lateral ischemic boundary. In the context of simulations of activation, Colli Franzone *et al.*[1] noted an identical change in pattern (with reversed polarities) as an activation wave front moved from the endocardium to the epicardium. As we will discuss below, during ischemia of modest transmural extent, primary sources of injury current lie at the transmural border while with more extensive extent of ischemia, the primary sources move to the lateral borders.

Over the ranges we explored, conductivity values did not drastically affect epicardial potential patterns at medium and high extents of transmural ischemia. In the case of 70% ischemia, Fig. 6 shows a central maximum flanked by two minima at all conductivity values; changes in the conductivity values affected only the magnitudes of the extrema. Similarly, Colli Franzone *et al.*[1] found that the tripolar pattern persisted throughout a range of intracellular anisotropy values and blood conductivity values, at least when an activation wave front was fairly near the epicardial surface, a situation that corresponds to thick ischemia. At 10% ischemia, changes in conductivity mainly affected the magnitudes of the epicardial potentials but also changed the epicardial patterns somewhat. For example, as shown in Fig. 4, a change in the intracellular anisotropy ratio from 20 to 50 shifted the relative minimum from over the ischemic area to an area over the basal ischemic boundary.

Generally, the effects of conductivity changes on potential magnitudes depended on the predominant potential

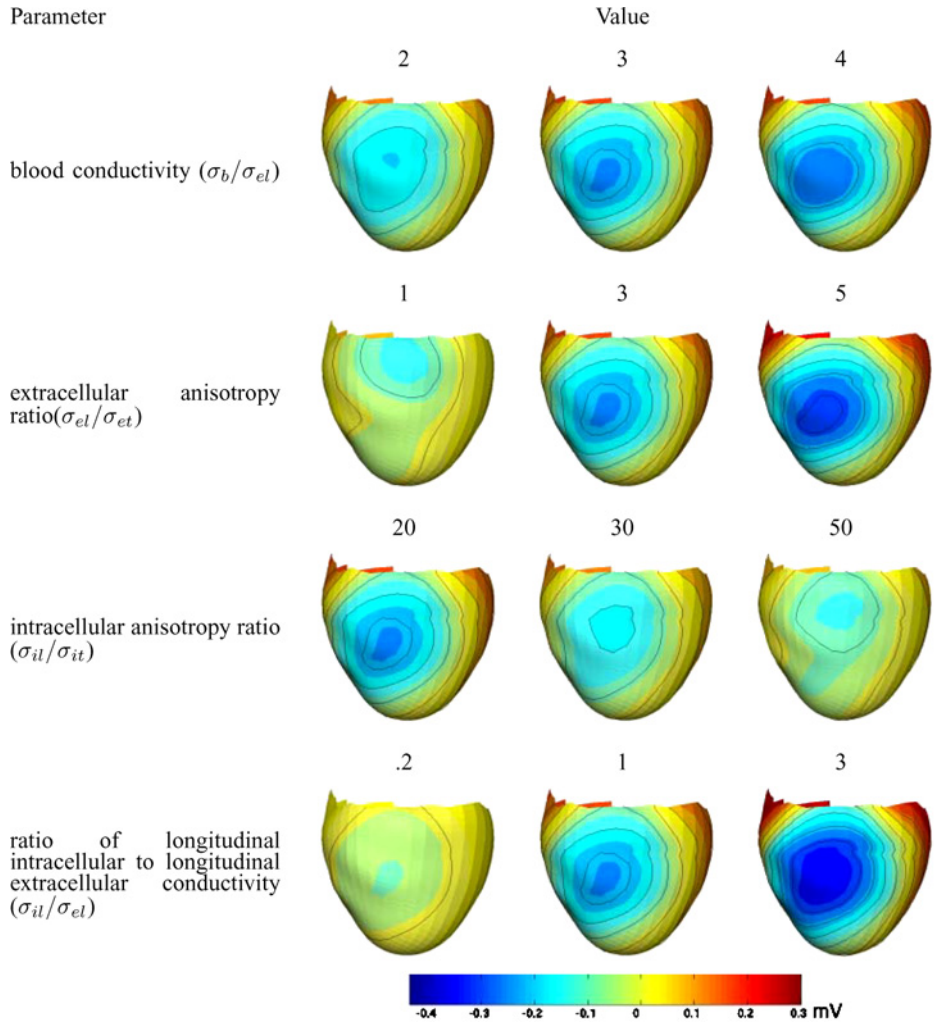

FIGURE 4. Epicardial distributions corresponding to different conductivity parameter values at 10% ischemia. Except as otherwise shown in the Figure, the parameter values are: blood conductivity (σ_b/σ_{el}) = 3; extracellular anisotropy ratio (σ_{el}/σ_{et}) = 3; intracellular anisotropy ratio (σ_{il}/σ_{it}) = 20; longitudinal intracellular conductivity to longitudinal extracellular anisotropy ratio (σ_{il}/σ_{el}) = 1.

source direction, lateral (40 and 70% ischemia) or transmural (10% ischemia). In particular, a comparison of Figs. 4 and 6, shows that an increase in the blood conductivity σ_b/σ_{el} or the extracellular anisotropy ratio σ_{el}/σ_{et} tended to result in an increase of the epicardial potential magnitudes at 10% ischemia but a decrease in the epicardial potential magnitudes at higher degrees of ischemia. (As alluded to in the Introduction, the longitudinal conductivities σ_{el} and σ_{il} primarily affect the lateral sources while the transverse conductivities σ_{et} and σ_{it} primarily affect the transmural sources.) Conversely, an increase in the intracellular anisotropy ratio σ_{il}/σ_{it} resulted in a decrease of the epicardial potential magnitudes at 10% ischemia but an increase in the epicardial potential magnitudes at higher percentages of ischemia. However, at all degrees of transmural ischemia, an increase in σ_{il}/σ_{el}, which corresponded to the overall intracellular to extracellular conductivity, resulted in an increase of the epicardial potential magnitudes.

Thickness of Ischemic Zone

Another finding that is visible in Figs. 4 and 6 and supported by many more simulations is that the overall magnitude of epicardial potentials resulting from ischemia grew with the extent of ischemia. Potential values at 10% ischemia were in the range of ± 0.5 mV (epicardial potential differences ≈ 1 mV) and grew to ± 3–5 mV (epicardial potential differences ≈ 10 mV) at 70% ischemia.

Role of the Volume Conductor Conductivity

We ran simulations at 40 and 70% ischemia in which the conductivity outside the ischemic and source regions

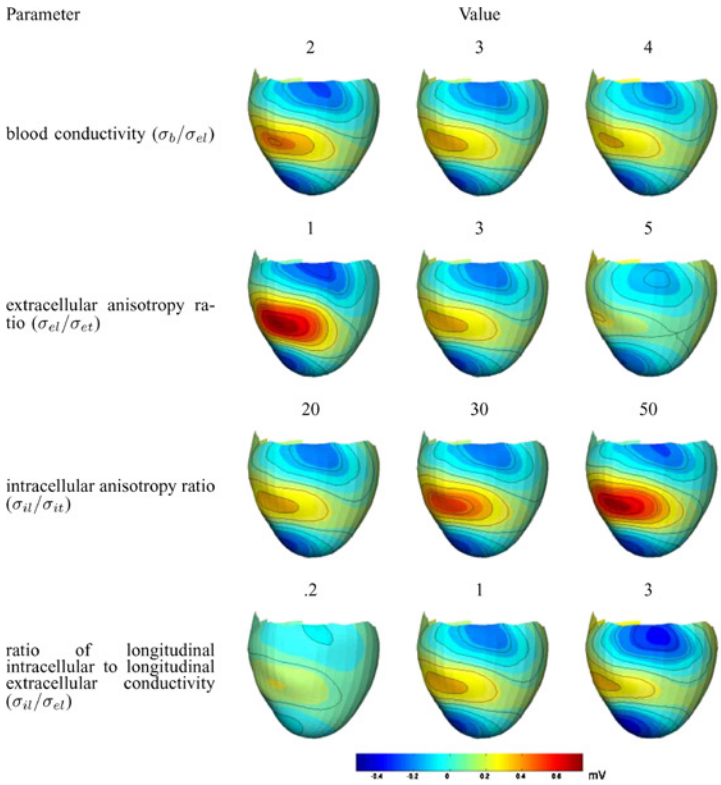

FIGURE 5. Epicardial distributions corresponding to different conductivity parameter values at 40% ischemia. Baseline parameter values are identical to those listed in the caption to Fig. 4.

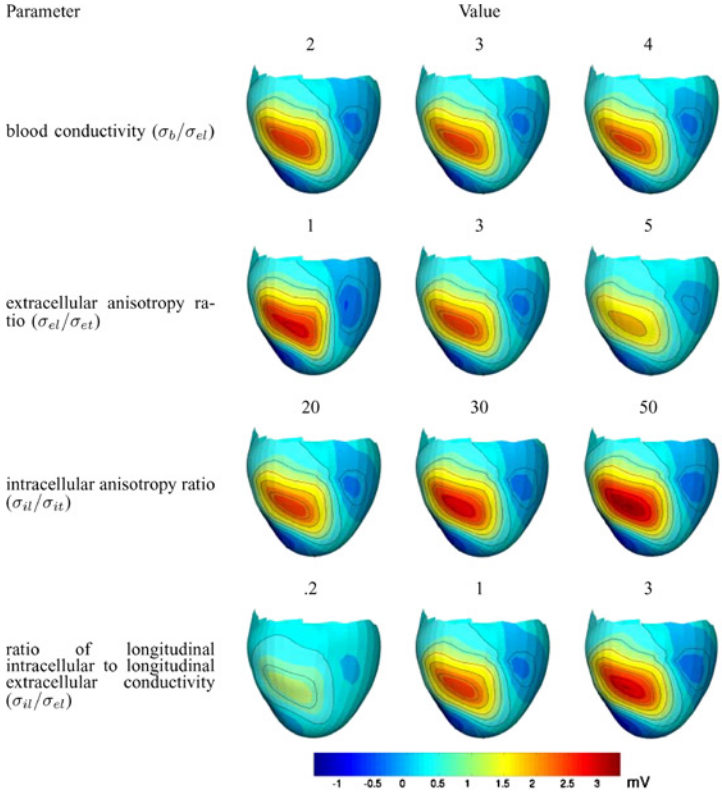

FIGURE 6. Epicardial distributions corresponding to different conductivity parameter values at 70% ischemia. Baseline parameter values are identical to those listed in the caption to Fig. 4.

was changed from baseline anisotropic values to isotropic values, while the conductivity of the source and ischemic regions was kept at baseline values. The results (not shown) suggested that both in the presence and absence of ventricular blood, the change from anisotropic to isotropic conductivity of the healthy heart tissue outside of the source region did not significantly alter the epicardial potential pattern but modestly decreased the magnitudes of the epicardial potentials. These results suggest that epicardial potentials are more sensitive to voltage source effects than secondary volume conductor effects.

Variation in Epicardial Potential Difference

Another metric we used to summarize the relationship between epicardial potentials and conductivities was the epicardial potential difference, i.e., the difference between the maximum and minimum of the epicardial potentials. Figure 7 shows the epicardial potential difference at 10% ischemia as a function of the transverse voltage source strength, i.e., Eq. (3), along with a linear regression line through the data. As shown, there is a reasonably linear relationship between the epicardial potential difference and the transverse voltage source strength, [Eq. (3)]. The motivation for plotting the epicardial potential as a function of the transverse source strength at 10% ischemia will be apparent from the Discussion section.

Figure 8 shows the epicardial potential difference at 40% and 70% ischemia as a function of the difference between longitudinal and transverse potential source strengths i.e., the difference between Eq. (2) and (3) ($\Delta V_{e,lat} - \Delta V_{e,tm}$). The data is marked according to the value of σ_{il}/σ_{el}. Because the function $\Delta V_{e,lat} - \Delta V_{e,tm}$ is so fundamental to the biophysical explanation for ischemic potentials, we give it the name "Voltage Difference Function" and describe its importance in more detail below. At 70% ischemia, the relationship between the epicardial potential difference and the Voltage Difference Function was linear. At 40% ischemia, this relationship was reasonably linear, although the dispersion around the regression line was greater than at 70% ischemia.

At 40% ischemia, although the data disperses about the regression line, there is a stronger linear correlation between the Voltage Difference Function and the epicardial potential difference for any given value of σ_{il}/σ_{el} apart from 3.

At 10% ischemia, there was an overall weak, positive correlation between blood conductivity and the epicardial potential difference. However, for at least some sets of conductivity parameter values at 10% ischemia, the correlation was stronger than the overall weak relationship. For example, in the case where $\sigma_{il}/\sigma_{el} = 3$, $\sigma_{il}/\sigma_{it} = 20$, and $\sigma_{el}/\sigma_{et} = 5$, doubling σ_b/σ_{el} from 2 to 4 resulted in an approximately 25% relative increase in the epicardial potential difference. At 70% ischemia, changing the blood

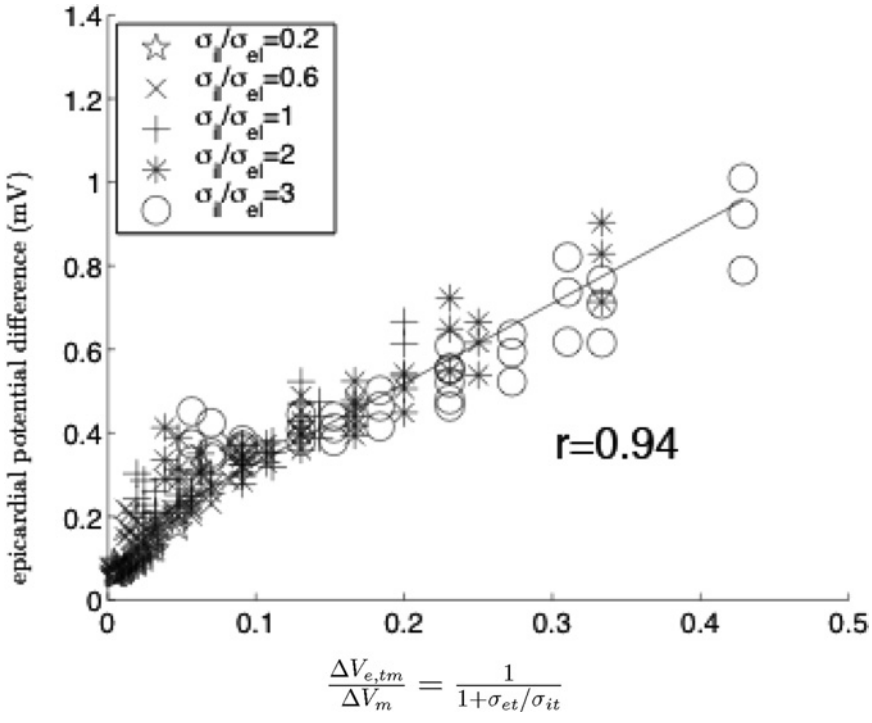

FIGURE 7. Epicardial potential difference at 10% ischemia as a function of the potential drop ($\Delta V_{e,tm}$), normalized for the transmembrane potential difference ($\Delta V_m = -30$ mV) between healthy and ischemic tissue, across a transmural boundary. A linear least squares regression line is shown.

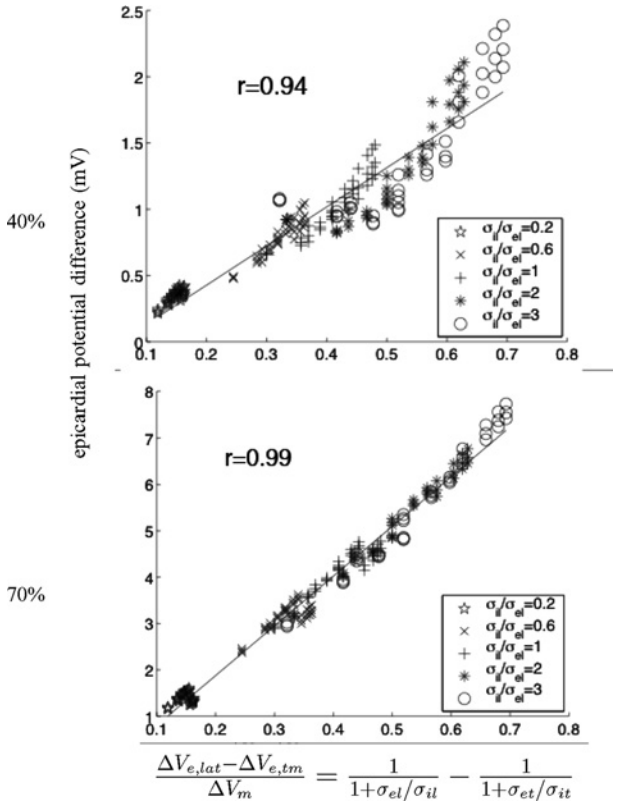

FIGURE 8. Epicardial potential difference at 40 and 70% ischemia as a function of the Voltage Difference Function ($\Delta V_{e,lat} - \Delta V_{e,tm}$), nonnalized for the transmembrane potential difference ($\Delta V_m = -30$ mV) between healthy and ischemic tissue. Linear least square regression lines are shown. The data points are delineated by the ratio σ_{il}/σ_{el}, which controls the overall voltage source strength across the ischemic boundary.

conductivity resulted in minor decreases of the epicardial potential difference. At 40% ischemia, there was a modest negative correlation between blood conductivity and the epicardial potential difference.

DISCUSSION

There are two, closely related facets of the results in this study that warrant special discussion. The first is the response of the model to variations in tissue and blood conductivities and the consequences for creating and using such models for simulating ischemia. The second is the striking and recurring difference in response of the model to ischemic zones with less than 20% of transmural extent and those with more than 30% extent. This latter facet is of special relevance to the biophysical mechanisms that appear to be central to the electrocardiographic response to ischemia.

Overview

Although it is difficult to summarize the complex response of epicardial potential distributions to variations in all the parameters of this study, there are some general findings that emerge. At 10% ischemia, according to Fig. 8, ST-segment depression was centered over the ischemic region and the epicardial potential difference was positively correlated with the potential drop across the transmural boundary, $\Delta V_{e,tm}$, which is a function of $1/(1 + \sigma_{et}/\sigma_{it})$. At 40% and 70% ischemia, ST-segment depression occurred over the lateral boundaries of the ischemic region, and the epicardial potential difference was positively correlated with the difference between the potential drops across the lateral and transmural boundaries, $\Delta V_{e,lat} - \Delta V_{e,tm}$. As will be explained below, the difference between the 10% case on the one hand, and the 40% and 70% cases on the other, is that transmurally oriented potential sources govern current flow at 10% ischemia whereas laterally oriented potential sources dominate at the other the larger thicknesses. In the context of simulations of activation, Colli Franzone *et al.*[1] noted this transition from transmural to lateral dominance as a propagating activation wave front moved from the endocardium to the epicardium.

Detailed Biophysical Explanation of Results

An explanation of the effects of conductivity on epicardial potential distributions requires an understanding of the current flow loops that arise during ischemia. There are two major types of current loops. One of them dominates at lower degrees of transmural ischemia (e.g. <20%) and the other dominates at higher degrees of transmural ischemia (e.g. >60%). At intermediate extents of ischemia, both types of current loop are present and the resulting potentials arise through their interplay. To illustrate these patterns, the top and middle panels of Fig. 9 show schematic diagrams of the current loops and corresponding simplified circuit diagrams that model a transverse cross section through the heart for the cases of 10 and 70% ischemia, respectively. The diagram for 40% ischemia, shown in the bottom panel of Fig. 9, reflects aspects of both the 10 and 70% cases.

At 10% ischemia, the currents that arise from lateral potential sources are small because of shunting by ventricular blood. In particular, for those portions of a lateral boundary that are near the endocardium, and are therefore near ventricular blood, the current path through the blood is in parallel with the current path through the extracellular heart muscle, so that the effective total conductivity is the sum of the conductivities of the extracellular heart muscle and ventricular blood. In this case, one can substitute $\sigma_{el} + \sigma_b$, for σ_{el} in Eq. (2) and write for the total effective voltage divider equation applied in the longitudinal direction:

$$\Delta V_{e,lat} \approx \frac{\Delta V_m}{1 + \sigma_{el}/\sigma_{il} + \sigma_b/\sigma_{il}} \tag{4}$$

where σ_b is the conductivity of the ventricular blood, $\Delta V_{e,lat}$ is the effective extracellular potential strength across the

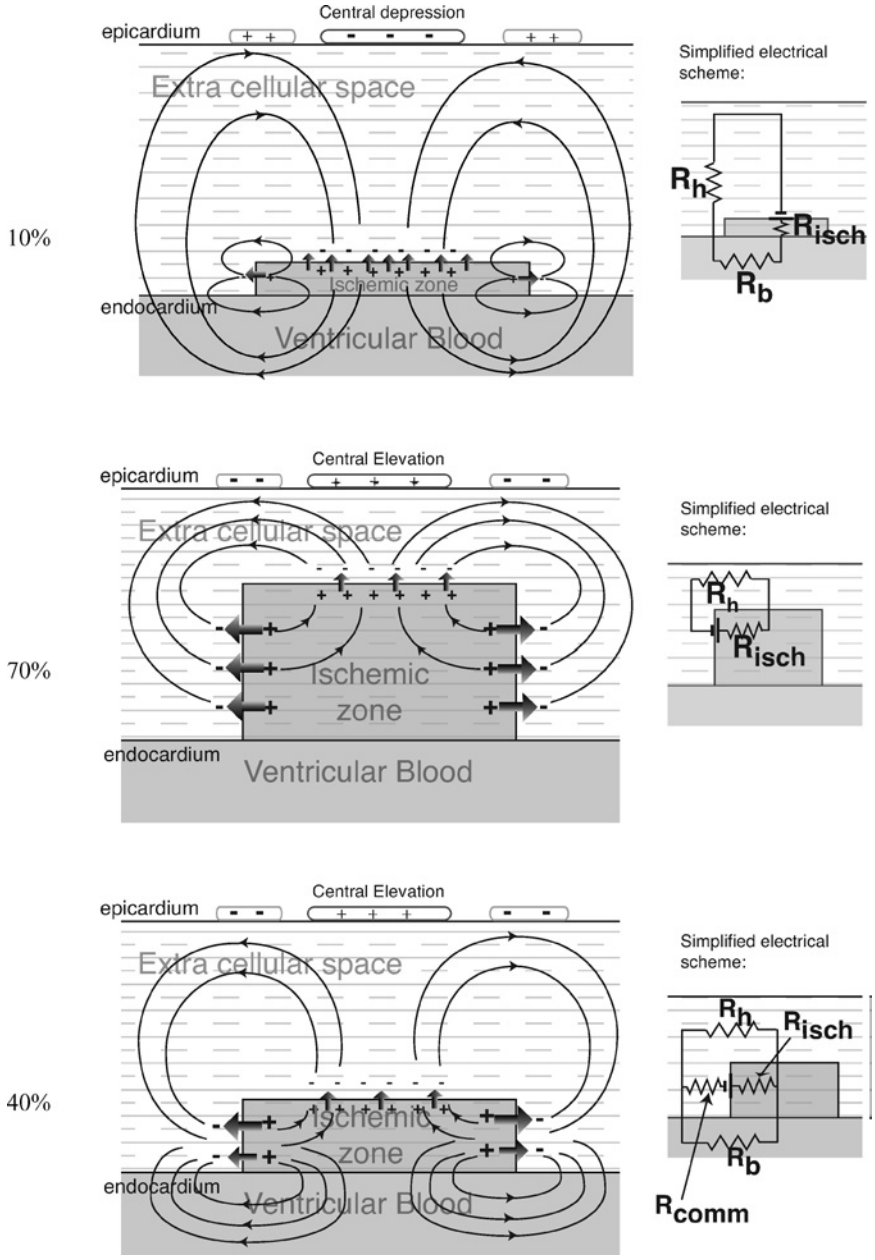

FIGURE 9. Current flow loops and corresponding circuit diagram models of the ventricles and blood at 10, 70, and 40% ischemia. R_h, R_b, and R_{isch} and are the resistances through portions of the healthy heart, ventricular blood, and ischemic patch, respectively. R_{comm} is the resistance through that portion of the healthy heart that is common to both current loops traveling through ventricular blood and from the epicardial side of the ischemic patch.

lateral boundary, and ΔV_m is the transmembrane potential difference between healthy and ischemic cells. The σ_b/σ_{il} term reduces $\Delta V_{e,lat}$. Indeed, at most sets of parameter values, $\Delta V_{e,lat}$ becomes smaller than the potential difference across the transmural boundary. Thus, transmurally oriented potential sources dominate.

The top panel of Fig. 9 illustrates schematically the large scale current loops that arise at 10% ischemia as a result of transmurally oriented potential sources. The figure shows the current from transmural sources that flows in a loop from the ischemic side of the transmural boundary, down through the ischemic tissue, then through the ventricular blood, and thence through the healthy tissue, along the epicardial surface, and then back to the healthy side of the transmural ischemic boundary. The epicardial potential difference ΔV_{epi}, is proportional to the potential difference through the healthy heart tissue, ΔV_h, which in turn is determined by the maximum potential difference across

the transmural boundary $\Delta V_{e,tm}$, and the resistances of the volume conductor, approximately according to a voltage divider equation as follows:

$$\Delta V_{epi} \sim \Delta V_h \approx \Delta V_{e,tm} \times \frac{R_h}{(R_{isch} + R_b + R_h)} \quad (5)$$

where R_h is the resistance through the healthy heart tissue, R_{isch} is the resistance through the ischemic tissue, and R_b is the resistance through the blood. R_h and R_{isch} are larger than R_b and hence determine ΔV_{epi} as indicated by the weak correlation between the epicardial potential difference and blood conductivity. Nonetheless, the enhancement of epicardial potentials associated with transmurally oriented sources is consistent with the Brody effect.[10] The resistance terms R_h and R_{isch} are functions of the bulk conductivity of cardiac tissue, which is determined by all four heart tissue conductivity values, σ_{il}, σ_{el}, σ_{it}, and σ_{et}.

The discussion thus far has been based on the assumption that fibers along the transmural ischemic border are perfectly parallel to that border, so that the potential drop across that border is solely a function of $\Delta V_{e,tm}$. In our computer heart model, however, the fibers along the transmural border are somewhat oblique, such that there is a longitudinal component to the potential drop across that border. This longitudinal component may explain most of the non-linearity in the plot shown in Fig. 7.

Some of the scatter in this plot is also attributable to the blood. According to Eq. (5), increases in blood conductivity, which correspond to decreases in R_b, would increase the epicardial potential difference.

The conditions that determine epicardial potentials are quite different for the case of thicker ischemia, as shown in the middle panel of Fig. 9. In this case, the potential difference ΔV_h across the healthy heart tissue may be estimated as follows:

$$\Delta V_{epi} \sim \Delta V_h \approx (\Delta V_{e,lat} - \Delta V_{e,tm}) \times \frac{R_h}{(R_h + R_{isch})}, \quad (6)$$

From the portions of the ischemic patch near the epicardium, the current path through the blood is very long and therefore so highly resistive that it may be regarded as an open circuit and thus ignored. The linearity of the plot in the second row, second column of Fig. 8 supports the hypothesis that, at large thicknesses of transmural ischemia, the epicardial potential difference is largely determined by the Voltage Difference Function.

Finally, for the case of medium thicknesses of ischemia, shown in the bottom panel of Fig. 9 for the case of 40% ischemia, the current loops represent an intermediate case between the 10 and 70% cases. On the one hand, as in the case of 10% ischemia, current loops through the blood can strongly affect epicardial potentials. On the other hand, as in the case of 70% ischemia, lateral potential sources generally dominate, which results in a central elevation over the ischemic patch flanked by two minima over the ischemic boundary.

Again, the potential difference across the epicardium ΔV_{epi} is proportional to the potential difference ΔV_h across the healthy heart tissue, which may be estimated as follows:

$$\Delta V_{epi} \sim \Delta V_h \approx (\Delta V_{e,lat} - \Delta V_{e,tm}) \times \frac{R_h}{R_h + R_{isch}} \times \frac{(R_h + R_{isch}) \| (R_b + R_{isch})}{(R_h + R_{isch}) \| (R_b + R_{isch}) + R_{comm}}, \quad (7)$$

where $\Delta V_{e,tm}$ is the potential difference across the transmural boundary, $\Delta V_{e,lat}$ is the maximum potential difference across a lateral boundary, R_h is the resistance through the healthy heart tissue, R_{isch} is the resistance through the ischemic tissue, and R_b is the resistance of the current path through the ventricular blood. From this relationship, ΔV_{epi} is an increasing function of ventricular blood resistance R_b.

Thus, at medium thicknesses of ischemia, increases in blood conductivity, which correspond to decreases in R_b, should decrease the epicardial potential difference. This was the case in the simulations discussed in this paper. The diminishing of epicardial potentials associated with laterally oriented sources is consistent with the Brody effect.[10] The effect of blood also partly explains the increased dispersion in the plot in the first row of Fig. 8.

To summarize

(1) At low thicknesses of ischemia (<20 %), ST-segment depression is centered over the ischemic region but is very small in magnitude. Transmural potential sources dominate current flow, such that the epicardial potential difference increases as a result of increases in (i) $\Delta V_{e,tm}$ and therefore increases in σ_{it}/σ_{et}; and (ii) blood conductivity.

(2) At large thicknesses of ischemia (>60 %), ST-segment elevation is centered over the ischemic region and is flanked by two depressions over the ischemic boundary. Lateral potential sources dominate the current flow, such that the epicardial potential difference increases as a result of (i) increases in $\Delta V_{e,lat}$, and therefore increases in σ_{il}/σ_{el} and (ii) decreases in $\Delta V_{e,tm}$. Since the top of the ischemic patch is relatively near the epicardium, blood has a minor effect on the epicardial potential difference.

(3) At medium thicknesses of ischemia (>30% and <50%), the epicardial patterns are generally similar to those at large thicknesses of ischemia. Lateral potential sources dominate current flow, such that the effect of the bidomain conductivities on the epicardial potential difference is similar to the case of large

thicknesses of ischemia. However, since all of the ischemic patch is relatively close to ventricular blood, blood conductivity can have a substantial effect on the epicardial potential difference.

Percentage thicknesses not included in the above summary are mixed cases. For example, 25% thickness ischemia is a hybrid of low and medium thickness ischemia.

In our simulations, the epicardium was insulated whereas in normal physiological conditions, the epicardium is electrically loaded by a torso, which may be expected to affect epicardial potentials. Li *et al*.[4] found that electrical insulation of the epicardium increased the magnitude of epicardial potentials but did not significantly alter the potential patterns. Thus, we believe that torso loading effects would not have substantially altered the epicardial potential patterns resulting from our simulations.

The simulated epicardial potentials do not completely match the epicardial potentials observed in an in situ sheep preparation as described in Li *et al*.[4] In particular, in the simulated results, ST elevation occurred at less than 70% thickness ischemia whereas Li *et al*.[4] observed elevation only when the ischemia was nearly completely transmural. There are at least two possible explanations for the discrepancy. First, it is possible that the heart is more electrically isotropic than the maximum degree of isotropy involved in our simulations. Greater isotropy means that the voltage drops across the lateral and transmural boundaries are more nearly equal, so that ST elevation occurs at larger thickness of ischemia compared to our simulations. Another possibility is that the epicardial potentials are sensitive to the difference in ischemic geometries between the present simulations and the experiments of Li *et al*.

Indeed, the relationship between conductivity values and epicardial potentials depends on the transmembrane potential profile within the ischemic region and the geometry of the ischemic region, which are generally more complicated than the simple patch described in this paper. We performed simulations with another type of geometry, in which the ischemic region comprised a spherical cap, and found that the relationship between the Voltage Difference Function and the epicardial potential difference was generally linear. However, we cannot assert that this generally linear relationship holds over all types of ischemic geometries and transmembrane potential distributions. Finally, the conductivity of the ischemic region is likely different than the conductivity of the healthy region;[9] we did not simulate this effect. Nonetheless, we believe the principles described in this paper will help to inform the relationship between conductivity and extracellular potentials in the case of these more complex situations.

CONCLUSION

The main finding of this study is that, over a wide range of conductivity values, ST-segment depression occurs over a lateral boundary between healthy and ischemic tissue, at least in the case of medium or thick ischemia. At large thicknesses of ischemia, the epicardial potentials exhibit a tripolar epicardial potential pattern—a central maxima flanked by two minima that rotated in a clockwise direction as ischemia became increasingly transmural.[2] At medium thicknesses of ischemia, this tripolar pattern occurs unless the extracellular anisotropy ratio is relatively large (>3).

Because we did not link the heart model to a torso, we cannot hypothesize whether the same epicardial potential patterns will be manifest on the body surface. The detectability of these patterns depends on the magnitudes of the epicardial potentials but also on the effects of the torso volume conductor. Thus, the question of whether these patterns might serve as a diagnostically meaningful marker of ischemia is best addressed by body surface mapping studies[6] coupled with a forward solution approach that relates body surface potentials to epicardial potentials. Such studies may also have important consequences for developing inverse solution strategies that seek to localize ischemia based on body surface ECGs.[5]

ACKNOWLEDGMENTS

Support for this research comes from the Whitaker Foundation, the NIH/BISTI through the Program of Excellence for Computational Bioimaging and Visualization, and the Nora Eccles Treadwell Foundation.

REFERENCES

[1]Franzone, P., L. Colli, Guerri, M. Pennacchio, and B. Taccardi. Spread of excitation in 3-d models of the anisotropic cardiac tissue, iii. effects of ventricular geometry and fiber structure on the potential distribution. *Math. Biosci*. 151:51–98, 1998.

[2]Hopenfeld, B., J. G. Stinstra, and R. S. MacLeod. Mechanism for ST depression associated with contiguous subendocardial ischemia. *J Cardiovasc. Electrophysiol*. 15:1200–1206, 2004.

[3]Johnston, P. R., and D. Kilpatrick. The effect of conductivity values on st segment shift in subendocardial ischaemia. *IEEE Trans. Biomed. Eng*. 50:150–158, 2003.

[4]Li, D., C. Y. Li, A. C. Yong, and D. Kilpatrick. Source of electrocardiograhpic ST changes in subendocardial ischemia. *Circ. Res*. 82:957–970, 1998.

[5]MacLeod, R. S., and D. H. Brooks. Recent progress in inverse problems in electrocardiology. *IEEE Eng. Med. Biol. Mag*. 17:73–83, 1998.

[6]Menown, I. B., R. S. Patterson, G. MacKenzie, and A. A. Adgey. Body-surface map models for early diagnosis of acute

myocardial infarction. *J. Electrocardiol* 31(Suppl.):180–188, 1998.

[7]Nielsen, P. M., I. J. LeGrice, B. H. Smaill, and P. J. Hunter. Mathematical model of geometry and fibrous structure of the heart. *Am. J. Physiol.* 260(4 Pt2):H1365–H1378, 1991.

[8]Roberts, D. E., L. T. Hersch, and A. M. Scher. Influence of cardiac fiber orientation on wavefront voltage, conduction velocity and tissue resistivity. *Circ. Res.* 44:701–712, 1979.

[9]Stinstra, J. G., B. Hopenfeld, and R. S. MacLeod. A model for the passive cardiac conductivity. *Int. J. Bioelectromagn.* 5(1):185–186, 2003.

[10]van Oosterom, A., and R. Plonsey. The brody effect revisited. *J. Electrocardiol.* 24:339–48, 1991.